NaturalResourcesfor Human Health

eISSN: 2583-1194

Original Research

Received 20 Aug 2026
Revised 17 Sep 2026
Accepted 05 Oct 2026

Natural Resources for Human Health 2026, Vol. 6 (23s): 1226–1239

KEYWORDS:
Mytilus by-products; metabolic syndrome; cardio-renal protection; oxidative stress; molecular docking.

Biomarker, Histopathological, and Molecular Evidence for Cardiac and Renal Protection by Mytilus Galloprovincialis By-product Meal

Mustapha Walid Otsmane[1]*, Sabrine Louala[1], Nabila Boukhari Benahmed Daidj[1,2]

[1] Laboratory of Clinical and Metabolic Nutrition, Faculty of Nature and Life Sciences, University of Oran 1 Ahmed Ben Bella, Oran 31000, Algeria.
[2]Higher School of Biological Sciences of Oran, BP 1042 Saim Mohamed, Cité Emir Abdelkader (EX-INESSMO), Oran 31000, Algeria.

ABSTRACT: Western diet-induced metabolic syndrome damages the heart and kidneys, yet organ-specific protective strategies derived from sustainable food by-products remain underexplored. This study evaluated the cardiac and renal effects of a mussel (Mytilus galloprovincialis) by-product meal (MBy) in a rat model of diet-induced metabolic syndrome. Wistar rats were assigned to a standard diet (C), a hypercaloric Western diet (WD), or a WD in which casein was fully replaced by MBy (WD+MBy) (n=8/group). Renal and cardiac function, hemodynamic, inflammatory, and oxidative stress parameters were measured, histopathological examination of the heart and kidney was performed, and molecular docking of MBy-derived taurine, glycine, eicosapentaenoic acid (EPA), and docosahexaenoic acid (DHA) against Keap1, heme oxygenase-1 (HO-1), and the omega-3 receptor FFAR4/GPR120 was carried out. WD feeding significantly increased blood pressure, relative heart and kidney weight, urinary markers of glomerular and tubular dysfunction, and cardiac and renal tumor necrosis factor-alpha (TNF-α), interleukin-6 (IL-6), and malondialdehyde content, while lowering tissue superoxide dismutase, catalase, glutathione peroxidase, and glutathione levels ($p<0.05$ vs. C); WD+MBy supplementation significantly attenuated most of these changes relative to WD. Histopathological examination showed tubular necrosis, intraluminal necrotic debris, tubular epithelial vacuolization, and Bowman's space dilation in WD kidneys, and cardiomyocyte vacuolization, pyknotic nuclei, hypertrophy, and myofiber dissociation in WD hearts, with a less severe pattern in WD+MBy. Docking yielded predicted binding poses ranging from -3.1 to -7.7 kcal/mol, with DHA showing the most favorable interaction with FFAR4. MBy supplementation confers cardio-renal protective effects in diet-induced metabolic syndrome, potentially involving redox-sensitive and lipid-sensing signaling pathways.

1. INTRODUCTION

Obesity and its associated metabolic syndrome have reached pandemic proportions worldwide, with global prevalence more than doubling between 2000 and 2023 to affect an estimated 1.54 billion adults, driven largely by the widespread adoption of energy-dense, high-fat, high-sugar "Western" dietary patterns (Noubiap et al., 2025). Beyond dyslipidemia, hyperglycemia, and hypertension, this cluster of metabolic disturbances is increasingly recognized as a direct driver of structural and functional damage to the heart and kidneys, with oxidative stress and chronic low-grade inflammation forming a self-amplifying loop that sustains tissue damage across multiple organs (Chanda et al., 2023).

In parallel, the valorization of seafood processing by-products has emerged as a sustainable strategy to recover nutritionally and biologically valuable fractions that would otherwise be discarded as waste, in line with circular blue-bioeconomy principles aimed at converting processing residues into functional food ingredients, nutraceuticals, and biomaterials (Sasidharan et al., 2023). Mussels (Mytilus galloprovincialis), among the most heavily farmed and processed bivalves in the Mediterranean basin, generate substantial quantities of by-products during routine processing undersized individuals, byssus threads, and the intervalve liquid released during shucking. These fractions are rich in essential amino acids, taurine, and long-chain polyunsaturated fatty acids, notably eicosapentaenoic acid (EPA) and docosahexaenoic acid (DHA), positioning them as candidate functional ingredients for metabolic health applications. A separate, dedicated study by our group had already established the broader bioactive potential of the exact MBy batch used here, covering its biochemical composition (amino acid and fatty acid profiles among other parameters), its in vitro antioxidant capacity (through DPPH radical-scavenging, ferric-reducing power, and total antioxidant capacity assays), a preliminary indication of anti-inflammatory potential (via inhibition of heat-induced protein denaturation), and its food-safety profile (Otsmane et al., 2026); taken together, this positioned the by-product not merely as a nutrient source but as a credible candidate bioactive ingredient in its own right.

Despite this potential, whether dietary supplementation with a mussel by-product meal (MBy) can protect the two organs most vulnerable to metabolic syndrome-associated damage the heart and the kidney has, to our knowledge, not yet been examined, nor have the tissue-specific biochemical and molecular mechanisms underlying such protection been characterized. Redox-sensitive and lipid-sensing pathways such as Kelch-like ECH-associated protein 1/nuclear factor erythroid 2-related factor 2/heme oxygenase-1 (Keap1/Nrf2/HO-1), a well-established therapeutic target for renal protection against oxidative injury (Nezu et al., 2017), and the free fatty acid receptor 4 (FFAR4/GPR120), the principal membrane receptor mediating the metabolic and anti-inflammatory effects of long-chain omega-3 fatty acids such as DHA (Yin et al., 2023), have recently been implicated in cardiac and renal protection against metabolic and oxidative insults, yet their relevance to marine by-product-derived bioactive compounds remains largely uncharacterized.

The present study therefore aimed to characterize, by histopathological examination, the cardiac and renal architecture of rats fed a Western diet with or without MBy supplementation; to evaluate a targeted panel of renal function, hemodynamic, and tissue-specific inflammatory and oxidative stress parameters in the heart and kidney; and to explore, through molecular docking, the potential interactions between MBy-derived amino acids and fatty acids and the Keap1, HO-1, and FFAR4/GPR120 targets as a mechanistic hypothesis for the observed cardio-renal effects.

2. MATERIALS AND METHODS

2.1 MBy preparation and compositional characterization

Mussel by-product flour (MBy) was obtained from *Mytilus galloprovincialis* processing residues undersized or broken specimens, intervalve liquid released during shucking, and byssus threads, shells being discarded collected over a two-week period (late April to early May 2024) at the port of Kristel, Oran, Algeria, and transported to the laboratory under refrigeration. After manual shucking to separate the retained fraction from the shells, the material was heat-treated (80–85 °C, 20 min) to coagulate the proteins, following the fish-meal manufacturing procedure described in Guillaume et al. (1999), adapted here for mussel by-products; this produced an initial separation between the coagulated solid phase and a liquid phase (water and oil), which was completed by pressing, with the solid residue recovered from centrifugation of the press liquor reincorporated into the solid fraction. The combined solid fraction was then oven-dried (40–45 °C, 24 h, residual moisture below 10%), ground, and sieved (250 µm) to obtain a homogeneous flour, which was stored at –80 °C until analysis.

Full nutritional profiling of this MBy batch amino acids and fatty acids alike had already been carried out as part of a separate biochemical and food-safety characterization of the same raw material (Otsmane et al., 2026), and is only summarized here for context. In that prior work, hydrolysis of the protein fraction (6 M HCl, 110 °C, 24 h, nitrogen atmosphere) followed by pre-column o-phthaldialdehyde derivatization and HPLC separation with fluorescence detection (Agilent 1260) gave the amino acid profile, with tryptophan handled on a separate aliquot via alkaline hydrolysis (Landry and Delhaye, 1992) since it does not survive acid hydrolysis intact; lipids, for their part, were recovered following Bligh and Dyer (1959), converted into fatty acid methyl esters per Morrison and Smith (1964), and separated by GC-MS/FID, which yielded the relative abundance of each fatty acid and allowed the atherogenicity, thrombogenicity, and omega-3 indices to be derived. The values reproduced in Table 1 (mean ± SD, n = 6 analytical replicates on a single homogenized batch) come from that

earlier work, not from new analyses performed here; we include them simply so the cardio-renal results below can be read against the composition of the material that produced them. The full proximate, mineral, and vitamin profile, together with the food-safety data, is reported in that source.

2.2 Animals, diets, and experimental groups

Male Wistar rats (4–5 weeks old, initial body weight 100 ± 20 g) were sourced from the Pasteur Institute of Algiers and acclimated for 14 days under standard housing conditions (23 ± 3 °C, 55 ± 5% relative humidity, 12 h/12 h light/dark cycle) with free access to food and water. The n = 8/group sample size followed common precedent in comparable rodent metabolic syndrome studies, without an a priori power calculation. Animals of comparable weight were individually weighed and identified, then randomly allocated by hand to a normocaloric control diet (C, n = 8; casein 200, corn starch 640, sunflower oil 50, agar-agar 50, mineral mix 40, vitamin mix 20 $g \cdot kg^{-1}$; 15.9 $MJ \cdot kg^{-1}$) or a hypercaloric Western diet (n = 16; sheep fat 90, used frying oil 140 [recovered after five successive potato-frying cycles at 180 °C, its lipid-oxidation level confirmed by TBARS before dietary use], sucrose 200, corn starch 260, agar-agar 50 $g \cdot kg^{-1}$; 19.7 $MJ \cdot kg^{-1}$), balancing baseline weight between arms for an 11-week metabolic syndrome induction phase. At the end of induction, the sixteen Western-diet rats were re-weighed and randomly split by hand, again balancing mean body weight between arms, into two subgroups (n = 8 each) for the following 4-week intervention phase: one continuing the unsupplemented Western diet (WD) and one receiving a WD formulation in which casein was fully substituted by MBy on an isoproteic/isolipidic/isoenergetic basis (WD+MBy; 19.7 $MJ \cdot kg^{-1}$, matched to WD), while the control group remained on its original diet throughout. Body weight was recorded weekly and food intake measured daily by differential weighing (± 0.1 g) to monitor animal health status throughout the protocol. No humane endpoints needed to be applied, as no animal displayed signs of severe distress during the study, and all 24 rats completed the protocol with no exclusions from the analyses. All procedures complied with European Directive 86/609/EEC and were approved by the Institutional Animal Ethics Committee of the University of Oran 1 Ahmed Ben Bella (approval No. 991).

2.3 Biochemical assays

Systolic and diastolic blood pressure and heart rate were recorded weekly by tail-cuff plethysmography (CODA system, Kent Scientific, USA), after the rats had been habituated to the restraint procedure and pre-warmed to ensure adequate tail blood flow. On day 28 of the intervention phase, rats fasted for 12 h were anaesthetised with chloral hydrate (10% w/v, 3 $mL \cdot kg^{-1}$, intraperitoneally), and blood was collected by aortic puncture into dry tubes before euthanasia by exsanguination. Blood was allowed to clot and centrifuged (3,000 × g, 20 min, 4 °C), and the serum was stored at −80 °C until analysis. The heart and kidneys were excised and weighed; one portion was was stored at −80 °C for the biochemical assays and the other was fixed in 10% buffered formalin for histology.

Frozen cardiac and renal tissue (1 g) was homogenised (1:10, w/v) in ice-cold phosphate-buffered saline (0.1 M, pH 7.4) and centrifuged (4,000 × g, 15 min, 4 °C); the supernatants were used for the tissue assays, and their protein content was measured by the Bradford method (Bradford, 1976) with bovine serum albumin as the standard, so that enzymatic activities could be expressed per mg of protein. Serum creatinine and urea were determined with commercial colorimetric reagents (Jaffé reaction for creatinine; enzymatic method for urea), and a complete urinary panel (diuresis, creatinine, albumin/microalbumin, total protein, glucose, electrolytes, phosphate) was obtained from urine collected in metabolic cages.

Cardiac and renal TNF-α and IL-6 concentrations were quantified in the tissue supernatants by sandwich enzyme-linked immunosorbent assay (ELISA) using commercial kits, following the manufacturers' instructions. Oxidative stress markers were measured spectrophotometrically: lipid peroxidation as malondialdehyde (MDA) reacting with thiobarbituric acid to form a pink adduct read at 532 nm (Ohkawa et al., 1979); catalase activity from the rate of hydrogen peroxide decomposition at 240 nm (Aebi, 1984); superoxide dismutase (SOD) activity from the inhibition of pyrogallol autoxidation at 440 nm (Marklund and Marklund, 1974); glutathione peroxidase (GPx) activity from the consumption of glutathione in the presence of hydrogen peroxide, the residual glutathione being quantified with 5,5'-dithiobis(2-nitrobenzoic acid) (DTNB) (Flohé and Günzler, 1984); and reduced glutathione (GSH) content by its reaction with DTNB (Sedlak and Lindsay, 1968).

2.4 Histopathological evaluation

Cardiac and renal specimens were fixed, paraffin-embedded, sectioned at 5 μm, stained with hematoxylin-eosin, and examined by light microscopy at ×400 magnification (n = 8 rats/group). Sections were assessed qualitatively and in a blinded manner for characteristic lesions tubular necrosis, intraluminal necrotic debris, tubular epithelial cytoplasmic vacuolization, and Bowman's space dilation in the kidney; cardiomyocyte cytoplasmic vacuolization, pyknotic nuclei, cellular hypertrophy, and myofiber dissociation in the heart.

2.5 Molecular docking analysis

Predicted interactions between MBy-derived taurine, glycine, EPA, and DHA and three cardio-renal protective targets heme oxygenase-1 (HO-1, PDB 1N45), Keap1 (PDB 2FLU), and the omega-3 fatty acid receptor FFAR4/GPR120 (PDB 8H4L) were explored by blind docking. Ligand structures were obtained from PubChem (Kim et al., 2023) and receptor structures from the RCSB Protein Data Bank (Burley et al., 2021). Docking was performed using CB-Dock2 (Liu et al., 2022), built on the AutoDock Vina scoring engine (Trott and Olson, 2010; Eberhardt et al., 2021), and the highest-scoring pose for each pair was visualized in BIOVIA Discovery Studio Visualizer, with protein–ligand interactions classified by bond type (conventional/carbon hydrogen bonds, van der Waals contacts, alkyl/π-alkyl interactions).

2.6 Statistical analysis

In vivo results are expressed as mean ± SEM (n = 8/group); compositional data for MBy (Table 1) are expressed as mean ± SD (n = 6 analytical replicates on a single homogenized batch), as previously reported for this material (Otsmane et al., 2026). Group comparisons were performed by one-way ANOVA followed by Tukey's post hoc test using IBM SPSS v27.0, and differences were considered statistically significant at $p<0.05$. In Tables 2 and 3, values in a row not sharing a superscript letter differ significantly ($p<0.05$).

3. RESULTS AND DISCUSSION

3.1 Compositional profile of MBy

Table 1 gives the amino acid and fatty acid profile we previously measured for this same MBy batch (Otsmane et al., 2026); we repeat it here only as a reference point for interpreting the cardio-renal results that follow. Of the quantified amino acid pool (taurine aside), roughly two-thirds was accounted for by non-essential residues (61.84 g/100 g protein, 63.8%) against 35.09 g/100 g protein (36.2%) for the nine indispensable ones, with glutamic acid, glycine, and aspartic acid together dominating the non-essential fraction and taurine itself reaching 2.31 g/100 g protein on top of the protein-bound total. On the lipid side, saturated fatty acids formed the largest class (42.35% of total fatty acids), ahead of the polyunsaturated (29.18%) and monounsaturated (27.89%) fractions; palmitic, oleic, and stearic acid were the leading contributors among individual fatty acids, while EPA led the long-chain PUFA subgroup specifically. Two derived indices point the same direction nutritionally: an n-6/n-3 ratio of 0.76, well under the 4:1 threshold generally considered unfavorable, and an omega-3 index of 11.61%, both consistent with and lending indirect support to the EPA/DHA-centered mechanistic hypotheses this study set out to test.

Table 1. Amino acid composition (g/100 g protein) and fatty acid composition (% of total identified fatty acids) of MBy, and derived lipid quality indices, as previously determined for this same batch (mean ± SD, n = 6 analytical replicates on a single homogenized batch; adapted from Otsmane et al., 2026).

Component	Content
Indispensable (essential) amino acids, g/100 g protein	
Histidine	1.83 ± 0.02
Threonine	2.96 ± 0.02
Valine	4.37 ± 0.04
Methionine	2.63 ± 0.02
Isoleucine	3.44 ± 0.02
Leucine	7.17 ± 0.05
Phenylalanine	4.86 ± 0.04

Lysine	6.93 ± 0.05
Tryptophan	0.90 ± 0.02
EAA subtotal	35.09 ± 0.28
Dispensable (non-essential) amino acids, g/100 g protein	
Aspartic acid	8.47 ± 0.05
Glutamic acid	13.14 ± 0.08
Serine	4.01 ± 0.03
Glycine	9.36 ± 0.06
Alanine	5.02 ± 0.04
Proline	7.90 ± 0.06
Tyrosine	3.37 ± 0.03
Cysteine	1.02 ± 0.01
Arginine	5.67 ± 0.04
Asparagine	1.79 ± 0.03
Glutamine	2.09 ± 0.03
NEAA subtotal	61.84 ± 0.46
Other / derived amino acid ratios	
Taurine	2.31 ± 0.03
BCAA (Leu+Ile+Val)	14.98 ± 0.11
Aromatic AA (Phe+Tyr+Trp)	9.13 ± 0.09
EAA/NEAA ratio	0.57
BCAA/AAA ratio	1.64
Saturated fatty acids (SFA), % total FA	
Myristic acid (C14:0)	3.59 ± 0.04
Pentadecanoic acid (C15:0)	0.54 ± 0.02
Palmitic acid (C16:0)	23.76 ± 0.18
Margaric acid (C17:0)	0.89 ± 0.01
Stearic acid (C18:0)	12.53 ± 0.12
Arachidic acid (C20:0)	0.43 ± 0.02
Heneicosanoic acid (C21:0)	0.17 ± 0.02
Behenic acid (C22:0)	0.24 ± 0.02
Lignoceric acid (C24:0)	0.20 ± 0.01
SFA subtotal	42.35 ± 0.44
Monounsaturated fatty acids (MUFA), % total FA	
Myristoleic acid (C14:1)	0.42 ± 0.01
Palmitoleic acid (C16:1)	4.82 ± 0.04
Oleic acid (C18:1n-9)	19.23 ± 0.14
Elaidic acid (C18:1n-9t)	0.37 ± 0.02
Gondoic acid (C20:1)	2.85 ± 0.02
Erucic acid (C22:1)	0.20 ± 0.02
MUFA subtotal	27.89 ± 0.25
Polyunsaturated fatty acids (PUFA), % total FA	
Linoleic acid (C18:2n-6)	3.58 ± 0.03
γ-Linolenic acid (C18:3n-6)	3.17 ± 0.03
α-Linolenic acid (C18:3n-3)	1.29 ± 0.01
Stearidonic acid (C18:4n-3)	0.64 ± 0.02
Eicosadienoic acid (C20:2)	2.05 ± 0.02
Eicosatrienoic acid (C20:3n-6)	1.48 ± 0.01
Arachidonic acid (C20:4n-6)	3.45 ± 0.03
EPA (C20:5n-3)	6.83 ± 0.04

DPA (C22:5n-3)	1.91 ± 0.02
DHA (C22:6n-3)	4.78 ± 0.04
PUFA subtotal	29.18 ± 0.25
Total identified fatty acids and derived indices	
Total identified fatty acids	99.42 ± 0.94
EPA + DHA	11.61 ± 0.08
Total n-3	15.45 ± 0.13
Total n-6	11.68 ± 0.10
n-6/n-3 ratio	0.76 ± 0.01
EPA/AA ratio	1.98 ± 0.03
PUFA/SFA ratio	0.69 ± 0.01
Omega-3 index (%)	11.61 ± 0.08
Atherogenicity index (AI)	0.69 ± 0.01
Thrombogenicity index (TI)	0.59 ± 0.01

EAA = essential (indispensable) amino acids; NEAA = non-essential (dispensable) amino acids; BCAA = branched-chain amino acids; AAA = aromatic amino acids; FA = fatty acids; AA = arachidonic acid (C20:4n-6); SFA = saturated fatty acids; MUFA = monounsaturated fatty acids; PUFA = polyunsaturated fatty acids; AI = atherogenicity index; TI = thrombogenicity index.

3.2 Renal function and cardiac hemodynamics

Renal and cardiac hemodynamic parameters are presented in Table 2. Relative to C, the WD group showed significantly higher serum and urinary creatinine, serum urea, and markedly elevated albuminuria, proteinuria, and microalbuminuria; WD+MBy values were intermediate between WD and C for all parameters, consistent with a partial but significant attenuation of WD-induced renal dysfunction. Systolic and diastolic blood pressure were likewise significantly higher in the WD group than in C, with intermediate, significantly improved values in WD+MBy, and absolute and relative heart and kidney weights followed the same pattern, with the highest values recorded in WD and partial, significant normalization in WD+MBy (Table 2).

Table 2. Renal function and urinary parameters, blood pressure, and absolute/relative heart and kidney weights (mean ± SEM, n = 8/group).

Parameter	C	WD	WD+MBy
Renal function and urinary parameters			
Serum creatinine (mg/dL)	0.96 ± 0.01^{c}	1.70 ± 0.02^{a}	1.23 ± 0.08^{b}
Serum urea (mg/dL)	21.95 ± 1.40^{b}	33.88 ± 2.43^{a}	25.21 ± 1.50^{b}
Urinary creatinine (mg/24h)	9.61 ± 0.89^{c}	19.89 ± 0.56^{a}	12.76 ± 0.76^{b}
Albuminuria (mg/24h)	4.17 ± 0.25^{c}	32.14 ± 2.24^{a}	15.46 ± 0.78^{b}
Proteinuria (mg/24h)	18.48 ± 0.86^{c}	97.31 ± 3.70^{a}	45.72 ± 2.35^{b}
Microalbuminuria (mg/24h)	0.035 ± 0.006^{c}	37.696 ± 2.130^{a}	25.027 ± 1.651^{b}
Cardiac hemodynamics and organ weights			
Systolic BP (mmHg)	116.68 ± 5.37^{b}	167.88 ± 8.97^{a}	139.68 ± 5.55^{b}
Diastolic BP (mmHg)	82.68 ± 5.73^{b}	129.78 ± 6.53^{a}	96.86 ± 3.09^{b}
Absolute heart weight (g)	0.72 ± 0.03^{b}	1.16 ± 0.08^{a}	0.87 ± 0.05^{b}
Absolute kidney weight (g)	1.37 ± 0.07^{c}	2.37 ± 0.06^{a}	1.92 ± 0.13^{b}
Relative heart weight (%)	0.225 ± 0.010^{b}	0.245 ± 0.020^{a}	0.215 ± 0.014^{b}
Relative kidney weight (%)	0.430 ± 0.018^{b}	0.503 ± 0.010^{a}	0.474 ± 0.025^{ab}

Values are mean ± SEM (n = 8/group). Values in a row not sharing a superscript letter differ significantly ($p < 0.05$; one-way ANOVA, Tukey's post hoc test). C: control; WD: Western diet; WD+MBy: Western diet + mussel by-product meal.

3.3 Tissue-specific inflammation and oxidative stress

Cardiac and renal TNF-α and IL-6 concentrations were significantly higher in WD than in C, with significant attenuation in WD+MBy. A consistent pattern was observed for cardiac and renal oxidative stress markers: MDA content was significantly

elevated in WD hearts and kidneys, while SOD, CAT, GPX, and GSH were significantly lower than in C; WD+MBy significantly restored these markers toward C values (Table 3).

Unlike the other oxidative stress markers, renal SOD activity in WD+MBy did not differ significantly from C, indicating full normalization for this parameter.

Table 3. Cardiac and renal TNF-α/IL-6 concentrations, and cardiac and renal oxidative stress markers (mean ± SEM, n = 8/group).

Parameter	C	WD	WD+MBy
Cytokines			
Cardiac TNF-α (pg/mg protein)	17.62 ± 1.57^{c}	147.13 ± 6.29^{a}	54.17 ± 1.55^{b}
Cardiac IL-6 (pg/mg protein)	50.96 ± 1.86^{c}	438.35 ± 14.79^{a}	123.59 ± 12.29^{b}
Renal TNF-α (pg/mg protein)	22.98 ± 1.56^{c}	188.28 ± 9.33^{a}	61.91 ± 4.85^{b}
Renal IL-6 (pg/mg protein)	61.76 ± 3.94^{b}	540.02 ± 53.02^{a}	171.38 ± 15.64^{b}
Cardiac oxidative stress markers			
Cardiac MDA (nmol/mg protein)	3.81 ± 0.20^{c}	10.32 ± 0.63^{a}	6.73 ± 1.01^{b}
Cardiac SOD (U/mg protein)	69.31 ± 3.54^{a}	22.25 ± 2.19^{c}	49.25 ± 5.54^{b}
Cardiac CAT (U/mg protein)	134.19 ± 7.96^{a}	40.68 ± 1.63^{c}	88.87 ± 3.33^{b}
Cardiac GPX (U/mg protein)	23.40 ± 1.76^{a}	9.41 ± 0.49^{c}	17.50 ± 0.53^{b}
Cardiac GSH (nmol/mg protein)	17.39 ± 1.51^{a}	7.49 ± 0.37^{c}	12.14 ± 1.12^{b}
Renal oxidative stress markers			
Renal MDA (nmol/mg protein)	2.28 ± 0.42^{a}	8.26 ± 0.83^{c}	5.12 ± 0.67^{b}
Renal SOD (U/mg protein)	21.78 ± 2.17^{a}	9.80 ± 0.77^{b}	18.01 ± 1.15^{a}
Renal CAT (U/mg protein)	108.69 ± 4.10^{a}	36.97 ± 1.04^{c}	87.38 ± 3.31^{b}
Renal GPX (U/mg protein)	26.54 ± 1.68^{a}	8.96 ± 0.27^{c}	16.45 ± 0.48^{b}
Renal GSH (nmol/mg protein)	16.82 ± 2.06^{a}	6.54 ± 0.18^{c}	11.29 ± 0.85^{b}

Values are mean ± SEM (n = 8/group). Values in a row not sharing a superscript letter differ significantly ($p < 0.05$; one-way ANOVA, Tukey's post hoc test). C: control; WD: Western diet; WD+MBy: Western diet + mussel by-product meal.

3.4 Histopathological findings

Kidney sections from WD rats displayed tubular necrosis, intraluminal necrotic debris, tubular epithelial cytoplasmic vacuolization, and dilated Bowman's space (Figure 1A), whereas WD+MBy (Figure 1B) and C (Figure 1C) sections showed a largely preserved tubular and glomerular architecture. Cardiac sections from WD rats showed cardiomyocyte cytoplasmic vacuolization, pyknotic nuclei, cellular hypertrophy, and myofiber dissociation (Figure 2A), with a less severe pattern in WD+MBy (Figure 2B) and a preserved myocardial architecture in C (Figure 2C).

NaturalResourcesfor
Human Health
eISSN: 2583-1194

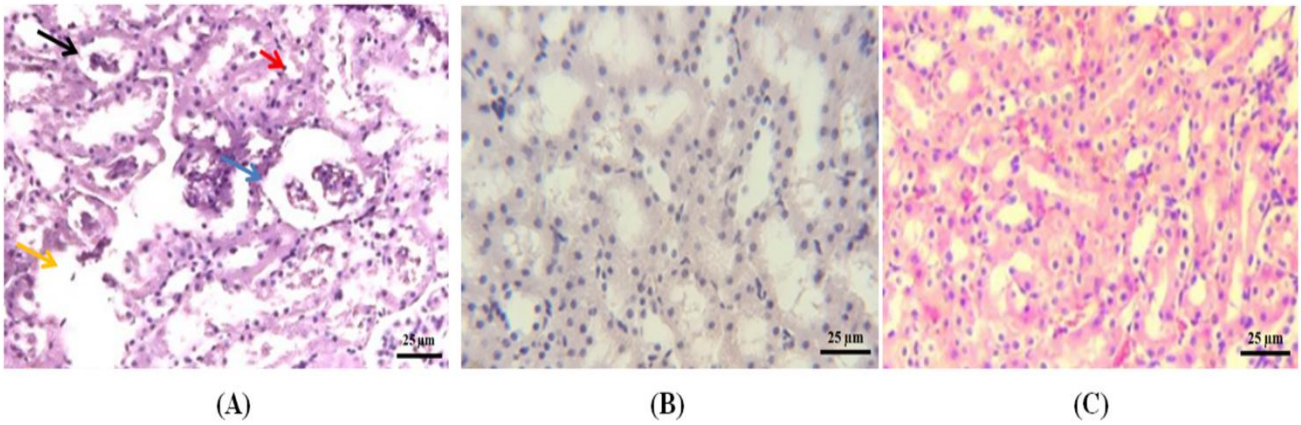


Figure 1. Representative photomicrographs of H&E-stained kidney sections (×400) from (A) WD, (B) WD+MBy, and (C) C rats. Arrows in (A): tubular necrosis (orange), intraluminal necrotic debris (black), tubular epithelial cytoplasmic vacuolization (red), dilated Bowman's space (blue). Scale bar = 25 µm.

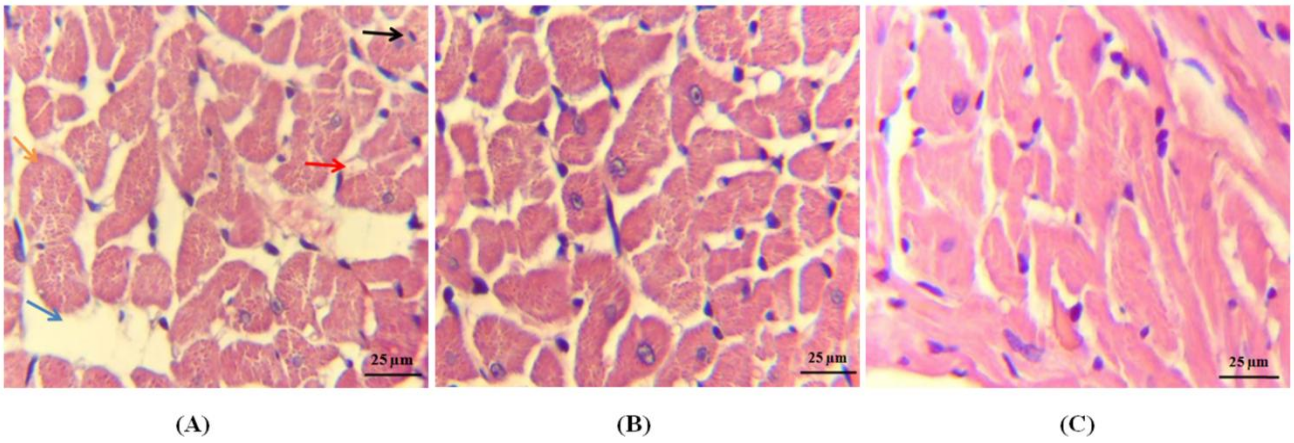


Figure 2. Representative photomicrographs of H&E-stained heart sections (×400) from (A) WD, (B) WD+MBy, and (C) C rats. Arrows in (A): cardiomyocyte cytoplasmic vacuolization (orange), pyknotic nuclei (black), cellular hypertrophy (red), myofiber dissociation (blue). Scale bar = 25 µm.

3.5 Molecular docking insights

Blind docking of MBy-derived taurine, glycine, EPA, and DHA against HO-1 (PDB 1N45), Keap1 (PDB 2FLU), and FFAR4/GPR120 (PDB 8H4L) yielded the following predicted binding affinities: taurine–HO-1, −3.8 kcal/mol; glycine–HO-1, −3.1 kcal/mol; taurine–Keap1, −4.3 kcal/mol; glycine–Keap1, −3.5 kcal/mol (Figure 3); EPA–FFAR4, −7.4 kcal/mol; and DHA–FFAR4, −7.7 kcal/mol, the most favorable pose overall (Figure 4). DHA showed a marginally more favorable predicted binding pocket than EPA on FFAR4, supported by an additional conventional hydrogen bond with Phe211. Both EPA and DHA formed a conventional hydrogen bond with Thr119 on FFAR4 while showing an unfavorable donor–donor interaction at Ser123, and were further stabilized by an extensive network of alkyl/π-alkyl contacts with hydrophobic residues (Phe, Leu, Ile, Val), consistent with a fatty-acid-binding pocket dominated by hydrophobic rather than polar interactions. On the polar targets, taurine consistently showed a more favorable predicted binding pocket than glycine on both HO-1 and Keap1, with Arg415 recurring as a hydrogen-bond anchor for both ligands on Keap1. These in silico observations are consistent with, but do not confirm, a mechanistic contribution of MBy-derived taurine, glycine, EPA, and DHA to the Keap1/Nrf2/HO-1 and FFAR4-mediated pathways underlying the cardio-renal findings described above.

NaturalResourcesfor
Human Health
eISSN: 2583-1194

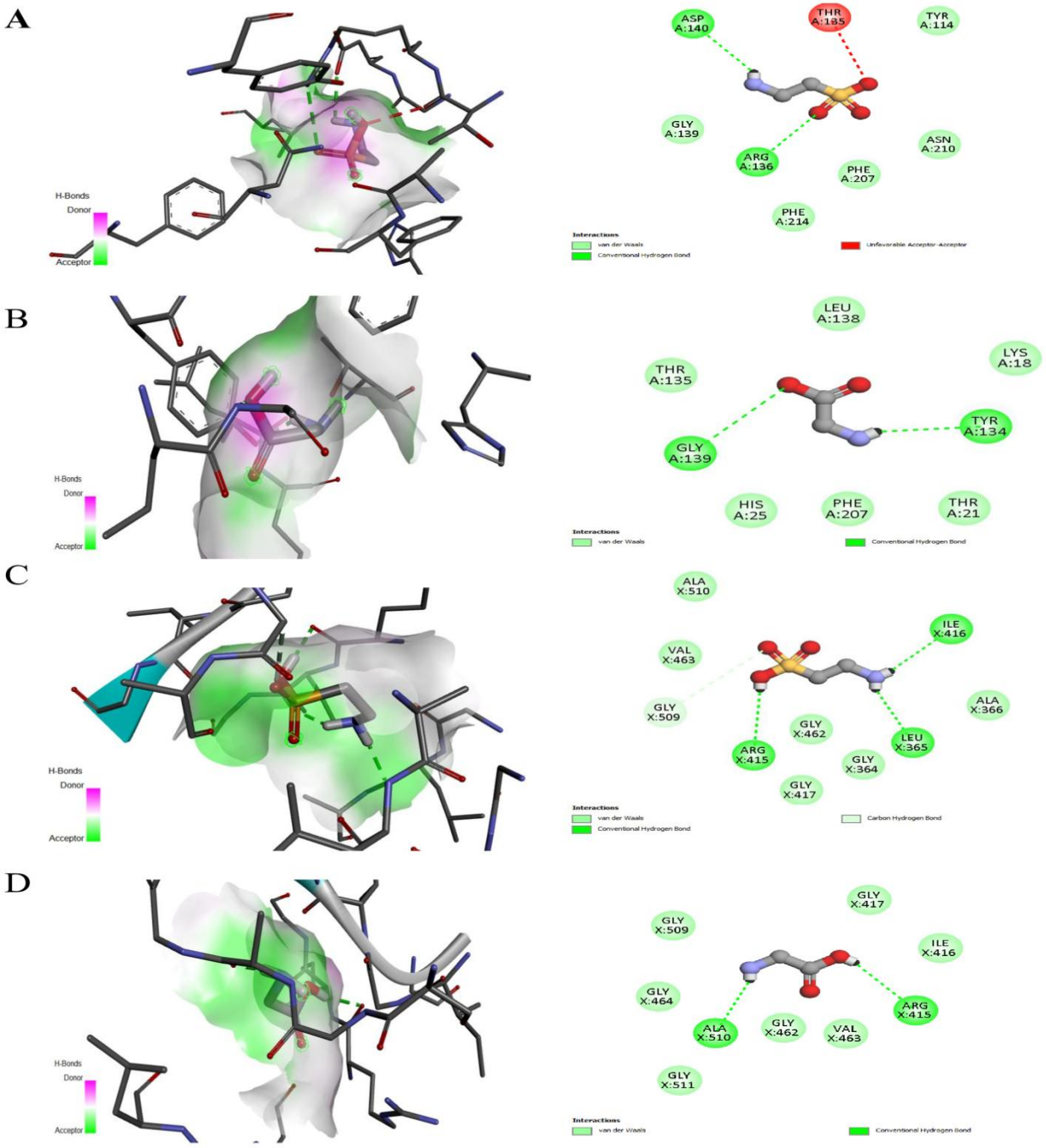


Figure 3. 2D and 3D predicted binding poses of (A) taurine–HO-1, (B) glycine–HO-1, (C) taurine–Keap1, and (D) glycine–Keap1, generated in BIOVIA Discovery Studio Visualizer.

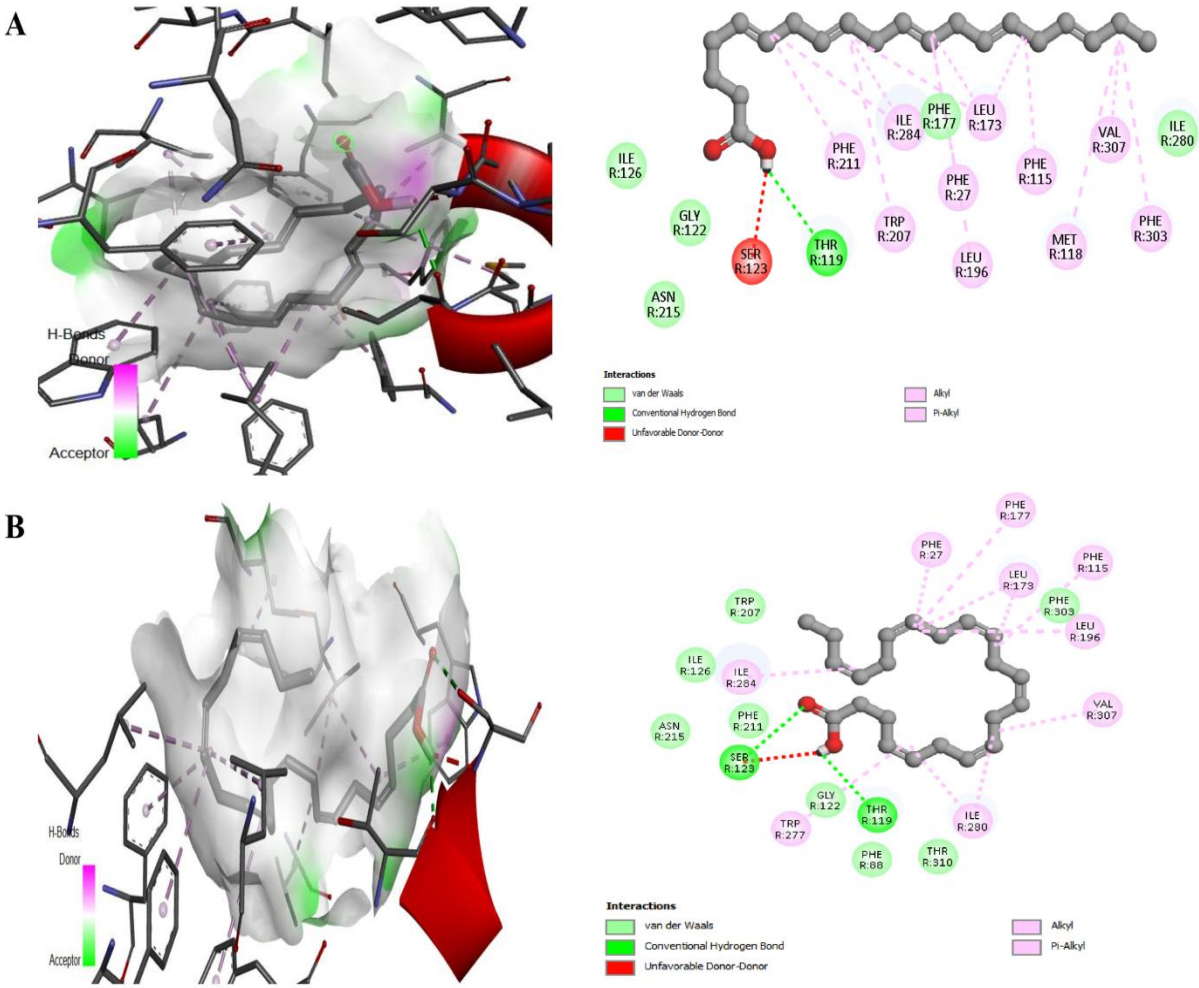


Figure 4. 2D and 3D predicted binding poses of (A) EPA–FFAR4/GPR120 and (B) DHA–FFAR4/GPR120, generated in BIOVIA Discovery Studio Visualizer.

3.4 Discussion

The pattern of renal and cardiac dysfunction observed in WD rats elevated blood pressure, organ hypertrophy, tubular and glomerular injury markers, and tissue-specific inflammation and oxidative stress is consistent with the broader recognition of the heart and kidney as principal targets of metabolic syndrome-associated damage, in which oxidative stress and chronic inflammation act as mutually reinforcing drivers of organ injury (Chanda et al., 2023). Excess reactive oxygen species in the kidney, generated predominantly through nicotinamide adenine dinucleotide phosphate (NADPH)-oxidase isoforms such as NOX-4, overwhelm enzymatic and non-enzymatic antioxidant defenses and drive tubular and glomerular injury (Simões e Silva, 2025), a mechanism consistent with the marked reduction in renal SOD, CAT, GPX, and GSH observed here in WD rats and their partial restoration with WD+MBy. A closely comparable pattern was reported for tuna protein hydrolysate in high-fat diet rats, where supplementation resolved hypertension and left ventricular hypertrophy alongside modulation of the renin-angiotensin system, oxidative stress, and the Nrf2/HO-1 axis (Maneesai et al., 2023), supporting the plausibility of a similar cardio-renal benefit for MBy-derived bioactive compounds in the present model.

At the cardiac level, the cardiomyocyte hypertrophy, pyknotic nuclei, and myofiber dissociation observed in WD hearts are consistent with the mechanistic link between mitochondrial dysfunction and NOD-, LRR- and pyrin domain-containing protein 3 (NLRP3) inflammasome activation increasingly implicated in pathological myocardial hypertrophy and heart failure progression (Yan et al., 2023), a pathway compatible with the markedly elevated cardiac TNF-α, IL-6, and MDA and reduced antioxidant enzyme activities seen in WD hearts. The partial normalization of these markers with WD+MBy parallels the

attenuation of cardiac hypertrophy and inflammatory markers reported for other marine-derived bioactive compounds in comparable high-fat/high-calorie rodent models (Maneesai et al., 2023).

The attenuation of renal injury markers and oxidative stress by MBy is consistent with documented protective mechanisms of its constituent amino acids: taurine modulates angiotensin II-driven NADPH oxidase activity and reinforces antioxidant enzyme responses in the kidney (Baliou et al., 2021), and has shown consistent anti-oxidative, anti-inflammatory, and anti-apoptotic effects in preclinical models of diabetic nephropathy (Ma et al., 2022); glycine, independently, exerts a well-characterized cytoprotective effect on renal tubular cells through inhibition of chloride channel-mediated cell injury during hypoxic and metabolic stress (Petrat et al., 2012). These established mechanisms provide biological plausibility for the improvements in renal function and tubular histology observed with WD+MBy relative to WD, and are broadly consistent with the protective role attributed to antioxidant micronutrients across renal oxidative stress conditions more generally (Dragoş et al., 2025).

The attenuation of cardiac and renal TNF-α and IL-6 by MBy is also mechanistically compatible with the original characterization of GPR120/FFAR4 as a functional omega-3 fatty acid receptor mediating potent anti-inflammatory effects in macrophages, whereby EPA and DHA binding suppresses pro-inflammatory cytokine production through this receptor (Oh et al., 2010). The molecular docking results offer a complementary, though exploratory, mechanistic hypothesis at the molecular target level. Keap1 is the principal negative regulator of Nrf2, and its inhibition is a well-established strategy for enhancing HO-1-mediated antioxidant defenses in the kidney (Nezu et al., 2017); the favorable predicted binding poses of taurine and glycine on Keap1, anchored by a hydrogen bond at Arg415, are consistent with a potential contribution of these MBy-derived amino acids to Nrf2 pathway modulation, compatible with the higher tissue GPX, CAT, and GSH levels observed in WD+MBy relative to WD. Similarly, FFAR4/GPR120 is the principal membrane receptor mediating the anti-inflammatory and metabolic actions of long-chain omega-3 fatty acids (Yin et al., 2023; Oh et al., 2010), and the strong predicted binding affinity of DHA and EPA for this receptor, stabilized mainly through hydrophobic and alkyl contacts typical of its fatty-acid-binding pocket, aligns with the attenuation of cardiac and renal TNF-α and IL-6 seen in WD+MBy. This is also consistent with the compositional profile of MBy itself (Table 1), whose favorable n-6/n-3 ratio and substantial EPA and DHA content provide a plausible dietary source for FFAR4 engagement.

Two methodological points qualify these conclusions. The docking results identify a plausible binding pocket on a static receptor structure; they do not establish that the predicted interactions actually occur in vivo, or that they drive the biochemical and histological changes observed, since neither receptor flexibility nor physiological ligand concentrations were modeled. The histopathological assessment, in turn, was descriptive rather than semi-quantitatively scored, which limits how far these structural observations can support causal interpretation on their own. On both counts, the docking results are best read as a mechanistic hypothesis compatible with the in vivo findings rather than as direct evidence of target engagement.

4. CONCLUSION

Beyond the organ-specific protective effects observed, this study provides evidence that a seafood by-product meal can simultaneously limit cardiac and renal damage in diet-induced metabolic syndrome while offering a plausible, target-level rationale for that protection, linking a circular blue-bioeconomy valorization strategy to redox-sensitive (Keap1/Nrf2/HO-1) and lipid-sensing (FFAR4/GPR120) pharmacology rather than to antioxidant activity alone. This reframes MBy not merely as a protein source but as a candidate multi-target cardio-renal nutraceutical, strengthening the case for repositioning an otherwise discarded processing residue as a functional food ingredient. Confirming this hypothesis will require site-directed mutagenesis or receptor-silencing studies to establish genuine target engagement, a dose–response trial to define the minimum effective MBy inclusion level, and longer-duration feeding studies to determine whether the partial renal and cardiac normalization observed here consolidates or diminishes with chronic exposure, before any human pilot evaluation in metabolic syndrome populations can be considered.

ACKNOWLEDGEMENTS

The authors wish to thank the laboratory personnel who assisted with the day-to-day animal husbandry and sample processing over the course of this study. This work was supported by the PRFU project of the Algerian Ministry of Higher Education and Scientific Research (grant number D00L01UN310120230001).

AUTHOR CONTRIBUTIONS

Mustapha Walid Otsmane: Conceptualization, Methodology, Investigation, Formal Analysis, Molecular Docking, Writing Original Draft.

Sabrine Louala: Conceptualization, Resources (provision of the rats), Methodology, Supervision, Writing, Review & Editing.

Nabila Boukhari Benahmed Daidj: Investigation (animal sacrifice procedures), Writing, Review & Editing.

All authors reviewed and approved the final manuscript.

CONFLICT OF INTEREST

The authors declare that there is no conflict of interest.

ETHICS STATEMENT

All procedures involving animals complied with European Directive 86/609/EEC and were approved by the Institutional Animal Ethics Committee of the University of Oran 1 Ahmed Ben Bella (approval No. 991).

DATA AVAILABILITY STATEMENT

The data supporting the findings of this study are available from the corresponding author upon reasonable request.

REFERENCES

[1] Aebi, H., 1984. Catalase in vitro. Methods in Enzymology 105, 121–126. https://doi.org/10.1016/S0076-6879(84)05016-3

[2] Baliou, S., Adamaki, M., Ioannou, P., Pappa, A., Panayiotidis, M., Spandidos, D., Christodoulou, I., Kyriakopoulos, A., Zoumpourlis, V., 2021. Protective role of taurine against oxidative stress (Review). Molecular Medicine Reports 24(2), 605. https://doi.org/10.3892/mmr.2021.12242

[3] Bligh, E.G., Dyer, W.J., 1959. A rapid method of total lipid extraction and purification. Canadian Journal of Biochemistry and Physiology 37(8), 911–917. https://doi.org/10.1139/y59-099

[4] Bradford, M.M., 1976. A rapid and sensitive method for the quantitation of microgram quantities of protein utilizing the principle of protein-dye binding. Analytical Biochemistry 72(1–2), 248–254. https://doi.org/10.1016/0003-2697(76)90527-3

[5] Burley, S.K., Bhikadiya, C., Bi, C., Bittrich, S., Chen, L., Crichlow, G.V., Christie, C.H., Dalenberg, K., Di Costanzo, L., Duarte, J.M., Dutta, S., Feng, Z., Ganesan, S., Goodsell, D.S., Ghosh, S., Green, R.K., Guranović, V., Guzenko, D., Hudson, B.P., ... Zhuravleva, M., 2021. RCSB Protein Data Bank: Powerful new tools for exploring 3D structures of biological macromolecules for basic and applied research and education in fundamental biology, biomedicine, biotechnology, bioengineering and energy sciences. Nucleic Acids Research 49(D1), D437–D451. https://doi.org/10.1093/nar/gkaa1038

[6] Chanda, D., Ha, H., Lee, I.K., 2023. Editorial: The role of oxidative stress and systemic inflammation in diabetes and chronic kidney disease. Frontiers in Endocrinology 14, 1272525. https://doi.org/10.3389/fendo.2023.1272525

[7] Dragoş, D., Enache, I.I., Manea, M.M., 2025. Oxidative stress and nutritional antioxidants in renal diseases: A narrative review. Antioxidants 14(7), 757. https://doi.org/10.3390/antiox14070757

[8] Eberhardt, J., Santos-Martins, D., Tillack, A.F., Forli, S., 2021. AutoDock Vina 1.2.0: New docking methods, expanded force field, and Python bindings. Journal of Chemical Information and Modeling 61(8), 3891–3898. https://doi.org/10.1021/acs.jcim.1c00203

[9] Flohé, L., Günzler, W.A., 1984. Assays of glutathione peroxidase. Methods in Enzymology 105, 114–120. https://doi.org/10.1016/S0076-6879(84)05015-1

[10] Guillaume, J., Kaushik, S., Bergot, P., Métailler, R., 1999. Fabrication des farines de poisson et contrôle de qualité: Principales matières premières d'origine animale [Manufacture of fish meal and quality control: Main raw materials of animal origin], in: Guillaume, J., Kaushik, S., Bergot, P., Métailler, R. (Eds.), Nutrition et alimentation des poissons et crustacés. INRA Éditions, pp. 346–351.

[11] Kim, S., Chen, J., Cheng, T., Gindulyte, A., He, J., He, S., Li, Q., Shoemaker, B.A., Thiessen, P.A., Yu, B., Zaslavsky, L., Zhang, J., Bolton, E.E., 2023. PubChem 2023 update. Nucleic Acids Research 51(D1), D1373–D1380. https://doi.org/10.1093/nar/gkac956

[12] Landry, J., Delhaye, S., 1992. Simplified procedure for the determination of tryptophan. Journal of Agricultural and Food Chemistry 40(5), 776–779.

[13] Liu, Y., Yang, X., Gan, J., Chen, S., Xiao, Z., Cao, Y., 2022. CB-Dock2: Improved protein–ligand blind docking by integrating cavity detection, docking and homologous template fitting. Nucleic Acids Research 50(W1), W159–W164. https://doi.org/10.1093/nar/gkac394

[14] Ma, J., Yang, Z., Jia, S., Yang, R., 2022. A systematic review of preclinical studies on the taurine role during diabetic nephropathy: Focused on anti-oxidative, anti-inflammation, and anti-apoptotic effects. Toxicology Mechanisms and Methods 32(6), 420–430. https://doi.org/10.1080/15376516.2021.2021579

[15] Maneesai, P., Wattanathorn, J., Potue, P., Khamseekaew, J., Rattanakanokchai, S., Thukham-Mee, W., Muchimapura, S., Pakdeechote, P., 2023. Cardiovascular complications are resolved by tuna protein hydrolysate supplementation in rats fed with a high-fat diet. Scientific Reports 13, 12280. https://doi.org/10.1038/s41598-023-39538-z

[16] Marklund, S., Marklund, G., 1974. Involvement of the superoxide anion radical in the autoxidation of pyrogallol and a convenient assay for superoxide dismutase. European Journal of Biochemistry 47(3), 469–474. https://doi.org/10.1111/j.1432-1033.1974.tb03714.x

[17] Morrison, W.R., Smith, L.M., 1964. Preparation of fatty acid methyl esters and dimethylacetals from lipids with boron fluoride–methanol. Journal of Lipid Research 5(4), 600–608. https://doi.org/10.1016/S0022-2275(20)40190-7

[18] Nezu, M., Suzuki, N., Yamamoto, M., 2017. Targeting the KEAP1-NRF2 system to prevent kidney disease progression. American Journal of Nephrology 45(6), 473–483. https://doi.org/10.1159/000475890

[19] Noubiap, J.J., Nansseu, J.R., Nyaga, U.F., Ndoadoumgue, A.L., Ngouo, A.T., Tounouga, D.N., Tianyi, F.L., Foka, A.J., Lontchi-Yimagou, E., Nkeck, J.R., Bigna, J.J., 2025. Worldwide trends in metabolic syndrome from 2000 to 2023: A systematic review and modelling analysis. Nature Communications 17(1), 573. https://doi.org/10.1038/s41467-025-67268-5

[20] Oh, D.Y., Talukdar, S., Bae, E.J., Imamura, T., Morinaga, H., Fan, W., Li, P., Lu, W.J., Watkins, S.M., Olefsky, J.M., 2010. GPR120 is an omega-3 fatty acid receptor mediating potent anti-inflammatory and insulin-sensitizing effects. Cell 142(5), 687–698. https://doi.org/10.1016/j.cell.2010.07.041

[21] Ohkawa, H., Ohishi, N., Yagi, K., 1979. Assay for lipid peroxides in animal tissues by thiobarbituric acid reaction. Analytical Biochemistry 95(2), 351–358. https://doi.org/10.1016/0003-2697(79)90738-3

[22] Otsmane, M.W., Louala, S., Krouf, D., Benhamou, H., Hakmi, A.A., Hassani, H., 2026. Valorization of Mytilus galloprovincialis processing by-products from the Southern Mediterranean: A preliminary single-site characterization of biochemical composition, in vitro bioactivity, and food safety. Egyptian Journal of Aquatic Biology and Fisheries 30(5), 1987–2016. https://doi.org/10.21608/ejabf.2026.505194.8227

[23] Petrat, F., Boengler, K., Schulz, R., de Groot, H., 2012. Glycine, a simple physiological compound protecting by yet puzzling mechanism(s) against ischaemia-reperfusion injury: Current knowledge. British Journal of Pharmacology 165(7), 2059–2072. https://doi.org/10.1111/j.1476-5381.2011.01711.x

[24] Sasidharan, A., Rustad, T., Cusimano, G.M., 2023. Tuna sidestream valorization: A circular blue bioeconomy approach. Environmental Science and Pollution Research 31, 62230–62248. https://doi.org/10.1007/s11356-023-28610-w

[25] Sedlak, J., Lindsay, R.H., 1968. Estimation of total, protein-bound, and nonprotein sulfhydryl groups in tissue with Ellman's reagent. Analytical Biochemistry 25, 192–205. https://doi.org/10.1016/0003-2697(68)90092-4

[26] Simões e Silva, A.C., 2025. Oxidative stress in renal health. Antioxidants 14(2), 144. https://doi.org/10.3390/antiox14020144

[27] Trott, O., Olson, A.J., 2010. AutoDock Vina: Improving the speed and accuracy of docking with a new scoring function, efficient optimization, and multithreading. Journal of Computational Chemistry 31(2), 455–461. https://doi.org/10.1002/jcc.21334

[28] Yan, R., Sun, Y., Yang, Y., Zhang, R., Jiang, Y., Meng, Y., 2023. Mitochondria and NLRP3 inflammasome in cardiac hypertrophy. Molecular and Cellular Biochemistry. Advance online publication. https://doi.org/10.1007/s11010-023-04812-1

[29] Yin, H., Inoue, A., Ma, Z., Zhu, X., Xia, R., Xu, Z., Wang, N., Duan, Y., Zhang, A., Guo, C., He, Y., 2023. Structural basis of omega-3 fatty acid receptor FFAR4 activation and G protein coupling selectivity. Cell Research 33(8), 644–647. https://doi.org/10.1038/s41422-023-00835-x